Second international spectroradiometer intercomparison: results and impact on PV device calibration

Roberto Galleano , Willem Zaaiman , Cecilia Strati , Simona Bartocci , Mauro Pravettoni , Matteo Marzoli , Raffaele Fucci , Gianni Leanza , Gianluca Timò , Alessandro Minuto , Mario Catena , Francesco Aleo , Shin Takagi , Akihito Akiyama , Rubén Nuñez and Giorgio Belluardo

ABSTRACT

This paper describes the results of an intercomparison of spectroradiometers for measuring global normal incidence and direct normal incidence spectral irradiance in the visible and in the near infrared, together with an assessment of the impact these results may have on the calibration of the short circuit current (I_{sc}) of triple-junction photovoltaic devices and on the relevant spectral mismatch calculation. The intercomparison was conducted by six European scientific laboratories and a Japanese industrial partner. Seven spectroradiometer systems, for a total of 13 different instruments/channels using two different technologies and made by four different manufacturers were involved. This group of systems represents a good cross section of the instrumentation for solar spectrum measurements available to date. The instruments were calibrated by each partner prior to the intercomparison following their usual procedure and traceability route in order to verify the entire measurement and traceability chain. The difference in measured spectral irradiance showed to have an impact on the calibration of a set of Iso-Type cells varying from ±2% to ±14% for middle and bottom cell, respectively.

KEYWORDS

solar radiation; solar cell; intercomparison; spectroradiometer; calibration

1. INTRODUCTION

The large variety of photovoltaic (PV) technologies available today on the market makes the measurement of the spectral content of the incoming sun light a key parameter for the characterization, calibration and energy yield estimation of these devices. Nowadays, spectroradiometers of different types (e.g., single-, double- stage rotating-grating monochromator or fixed single grating polychromator with photodiode array or CCD detectors) and of different manufacturing technologies are routinely used for measurements of solar spectra. So far, however, in the PV community, little attention has been paid to the evaluation of spectroradiometers performances and relevant measurement procedures to make solar spectrum measurements comparable and directly traceable to SI units [1–3]. In the framework of the European project "Apollon", an Italian project for the monitoring of the solar direct irradiance throughout the country and with the aim of sharing good laboratory practices and measurement procedures, a group of European research

institutes active in the PV research field, together with an industrial partner, set up the second intercomparison of spectroradiometers for solar spectrum measurements. The aims of the intercomparison were mainly to exchange and compare instrument calibration procedures, to assess spectroradiometer measurement capabilities under real working condition, establish equivalence figures for the measurements of solar spectra and to put in practice lessons learnt from the previous campaign. This paper describes the intercomparison campaign, reports on the results and analyzes a practical consequence that the differences in measured spectra may have on multi-junction PV device calibration.

2. EXPERIMENTAL SET UP AND APPROACH

The intercomparison took place at the "ENEL Ingegneria e Ricerca" laboratory in Catania (Italy) from 11 to 15 of June 2012. Seven spectroradiometer systems from four different manufacturers and representing two different technologies (single-stage rotating-grating and fast fixed-grating polychromator with photodiode or CCD array detectors) for a total of 13 different instruments were involved (some instruments were housed in a common chassis, however, consisting of two separate spectroradiometers). They were set to simultaneously measure global normal incidence (GNI) or direct normal incidence (DNI) spectral irradiance in the wavelength range from 360 to 1700 nm, depending on their entrance optics configuration. Table I summarizes the characteristics of the seven spectroradiometer systems, together with the relevant calibration chain. GNI spectral irradiance measurements were possible on six systems, and DNI spectral irradiance measurements were possible on five systems. These last allowed adding collimating tubes to their entrance optics in order to reduce the spectroradiometers' field of view to 5° nominal. Because of the differences among various instruments about measurement timing, bandwidth and spectral resolution, specific procedures for data acquisition and analysis were developed in order to make the spectroradiometers' output comparable. Details of the data acquisition and synchronization procedure were previously published [3]; here, we recall that we analyzed and compared an average spectrum, as result of several spectra acquired by "fast" polychromator, and one spectrum, as acquired by the slowest instrument, all measured during a 4-min acquisition time series. Within each time series, the irradiance must remain stable to 1% peak-to-peak or better to avoid adding errors arising from fast changing weather conditions affecting the output of spectroradiometers in different ways. For instance, for a "fast" polychromator, a thin cloud layer passing quickly close to the sun during the 4-min acquisition time may influence only few spectra that can be easily eliminated in the post processing phase. The same condition for a "slow" rotating-grating spectroradiometer may influence a part of the single spectrum acquired during the 4-min acquisition time and, thus, invalidate the entire measurement.

This constraint limited the useful sky conditions to clear or almost clear, discarding partially cloudy sky and measurements taken close to sunrise and sunset when the solar irradiance is fast changing. Because of the different instrument bandwidth and spectral resolution, all spectra were convoluted and interpolated in order to have spectral resolution of 2 nm and full width half maximum bandwidth of 8 nm. This step was useful to minimize artifacts when comparing results. Prior to the intercomparison, each participating laboratory calibrated their own spectroradiometer(s) following their usual procedures, thus allowing the evaluation of the whole instrument performance, including the traceability chain and the measurement procedures. Three spectroradiometer systems were calibrated by an external accredited calibration laboratory, two were in-house calibrated using standard lamps calibrated by accredited labs and two were calibrated at the manufacturer. All but one participant used accredited laboratories/standards for their systems calibration and, therefore, are directly traceable to SI units. All instruments were carefully aligned to point the sun when mounted on high-accuracy (±0.1°) solar trackers in order to reduce tracking errors, especially when measuring spectral DNI. During the 4-day intercomparison, clear- and cloudy-sky conditions were experienced, allowing for the evaluation

Table I. Summary of the characteristics of the spectroradiometers participating to the comparison.

Laboratory	Spectroradiometer	Detectors technology	Wavelength nm	Calibration chain
Supsi	EKO MS-710, MS-712	Si and InGaAs CCD Array	350–1700	In-house with calibrated standard lamp
JRC	Optronic Lab.OL 750	Single Si, PbS sandwich	350–2500	In-house with calibrated standard lamp
ENEA	StellarNet EPR2000NIR, EPP2000UV	2-CHs Si, InGaAs CCD array	250–1700	Accredited cal. Lab.
UniRoma	EKO MS-710, MS-712	Si and InGaAs CCD Array	350–1700	Factory calibrated
RSE	StellarNet EPR2000NIR, EPP2000UV	2-CHs Si, InGaAs CCD array	250–1700	Accredited cal. Lab.
EKO Japan ltd	EKO MS-710, MS-712	Si and InGaAs CCD Array	350–1700	Factory calibrated
ENEL	Aventes AvaSpec USB2	2-CHs Si + InGaAs CCD array	250–1700	Accredited cal. Lab.

of limitations in data comparison from such a diversity of instrument technologies. A set of triple-junction ISO-type cells was also measured during the intercomparison exercise in order to evaluate the impact on the cell calibration of using spectra measured at the same time by different instruments. In parallel to the intercomparison, a set of traceable calibrated shadowed pyranometers (for diffuse component) and cavity radiometers (for direct component) was also in use to acquire GNI and DNI reference irradiance data. The cavity radiometers assured the direct link to SI units for the irradiance quantity as they take part to the world radiometric intercomparison held every 5 years at PMOD-Davos (CH) [4]. For clear-sky conditions, the corresponding output data obtained from SMARTS model [5,6] were used for comparison purposes.

3. RESULTS OF THE INTERCOMPARISON, ANALYSIS AND DISCUSSION

3.1. Comparison of the acquired solar spectra

Because of good weather conditions during the intercomparison, the application of the irradiance stability acceptance limits to the measured spectral GNI and DNI resulted in a total of approximately 80 "stable" spectra. Figures 1–3 upper graphs show three stable data sets, out of 19, taken during a spectral DNI measurement session by the six partners' instruments equipped with collimating tubes. For comparison purposes, also the data obtained by running SMARTS code with actual local input parameters (time, temperature, atmospheric pressure, relative humidity and terrain type) are shown. Figures 1–3 report the second, fifth and eighteenth acquisition of the 4-h long session, respectively. The lower graphs in the same figures show the wavelength-by-wavelength per cent deviation of each spectrum with respect to Lab A spectrum and normalized to its peak irradiance. Lab A data were taken as reference because the instrument was running continuously during the comparison and has a characterized uncertainty. The average difference values for the measured spectra reported in Figure 1 are all positive and lay in a band of ±2% centered at 2.3% with associated standard deviations up to almost 9%. Three systems (Lab B, Lab E and Lab F) have most of their wavelength-by-wavelength difference values lying in a band of −5% to +10%, while Lab C and Lab D data show larger differences. The average difference values for the measured spectra reported in Figure 2 are all positive and lay in a band of ±2.3% centered at 3.1% with associated standard deviations up to 7.7%. Four systems (Lab B, Lab D, Lab E and Lab F) have most of their wavelength-by-wavelength difference values lying in a band of −5% to +15%, while Lab C data show larger differences. The average difference values for data reported in Figure 3 lay in a band of ±2.8% centered at 1.5% with associated standard deviations up to 7.1%. Wavelength-by-wavelength difference values show larger dispersion than the previous two data sets probably because of a drift of some instruments in pointing the sun occurred during the 4-h acquisition time window. As a confirmation of this assumption, upper graph in Figure 3 shows that Lab A and Lab D spectra have changed their relative position within the group in the wavelength band 360–950 nm and Lab E instrument further underestimates spectral irradiance above 800 nm.

Figures 4–6, upper, show three stable data sets relative to a spectral GNI acquisition obtained by the six partners' instruments equipped for this measurement. Also in this case, data obtained by running SMARTS code are shown. The lower graph in the same figures show the wavelength-

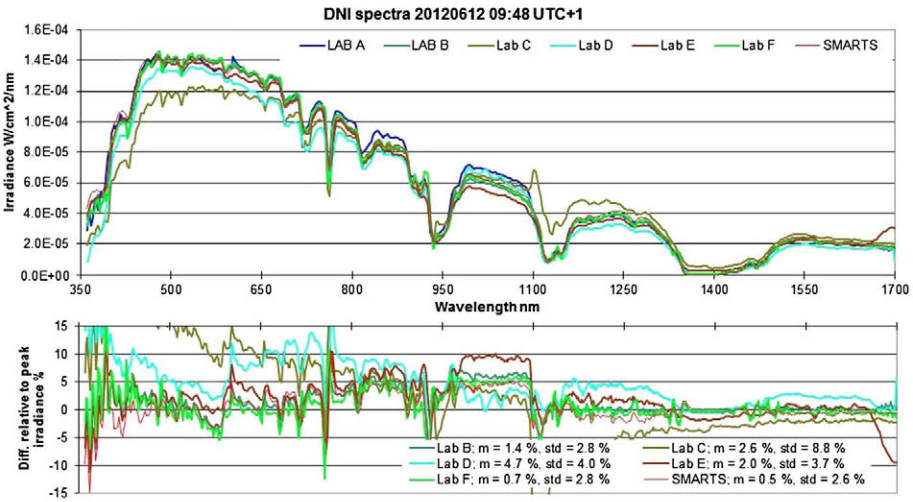

Figure 1. *Upper*: six DNI measured spectra plus spectrum obtained from the same time period by SMARTS code. *Lower*: wavelength-by-wavelength difference with respect to the Lab A spectrum and normalized to its peak irradiance; average and standard deviation calculated over the interval 360–1700 nm are also reported. These spectra were taken at the beginning of a 4-h long measurement session.

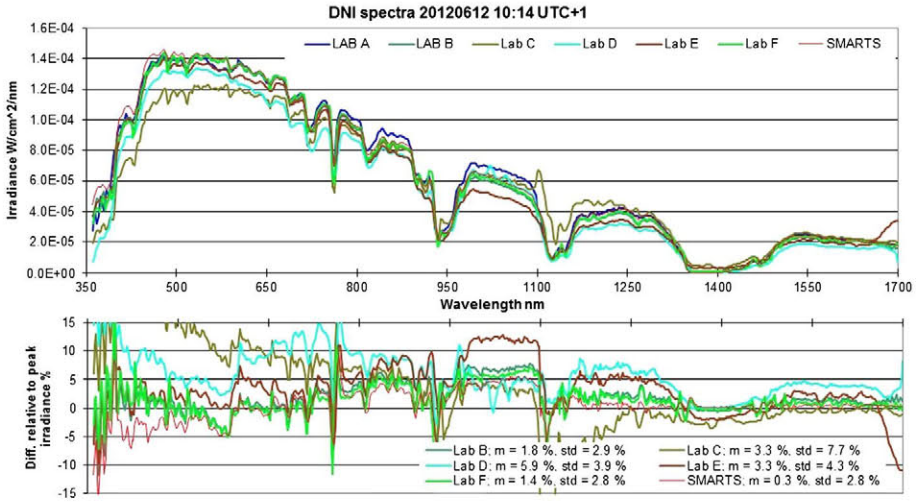

Figure 2. *Upper*: six DNI measured spectra plus spectrum obtained from the same time period by SMARTS code. *Lower*: wavelength-by-wavelength difference with respect to the Lab A spectrum and normalized to its peak irradiance; average and standard deviation calculated over the interval 360–1700 nm are also reported.

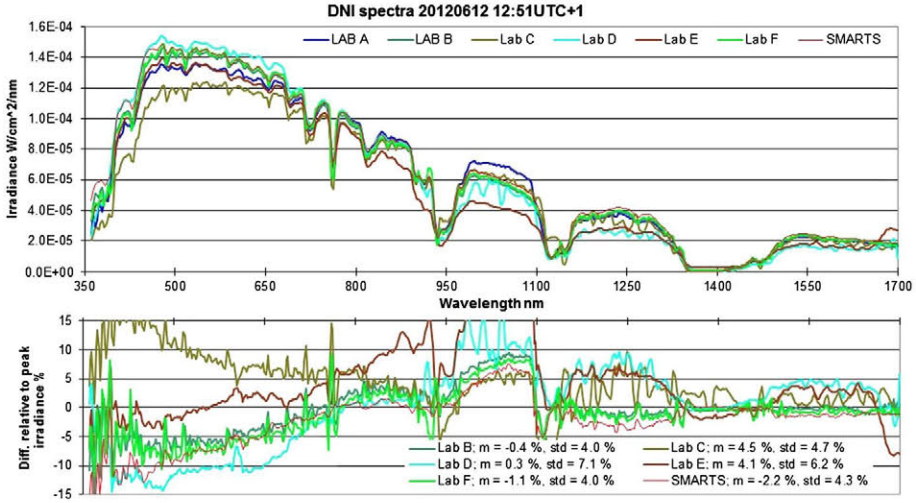

Figure 3. *Upper*: six DNI measured spectra plus spectrum obtained from the same time period by SMARTS code. *Lower*: wavelength-by-wavelength difference with respect to the Lab A spectrum and normalized to its peak irradiance; average and standard deviation calculated over the interval 360–1700 nm are also reported. These spectra were taken at the end of a 4-h long measurement session and show a different pattern probably due to pointing errors.

by-wavelength per cent deviation of each spectrum with respect to Lab A spectrum and normalized to its peak irradiance. Spectra reported in Figures 4–6 are the second, the eleventh and the twentieth in a series of 21 consecutive stable acquisitions, respectively. The sequence gives information on the measurement stability over approximately 4 h of acquisitions.

These graphs are representative of the entire measurement session and show similar patterns indicating a more stable situation with respect to the spectral DNI measurement session described before. Wavelength-by-wavelength difference plots show three instruments (Lab A, Lab B and Lab G) plus SMARTS model results agree to each other to within ±5% in the 400–1700 nm wavelength range. Two of the remaining instruments (Lab D and Lab E) show underestimation of the spectral irradiance in the 360–650 nm wavelength region varying from 5% to 15%. Lab F shows similar results to Lab D and Lab E but with an irradiance underestimation above 15% in the 400–500 nm region. The larger wavelength-by-wavelength differences found in analyzing spectral DNI data with respect to spectral GNI data may be partially explained by the non-uniform field of view among various instruments, by errors in pointing the systems at normal incidence and by mechanical misalignment of the spectroradiometers that occurred during the measurement session.

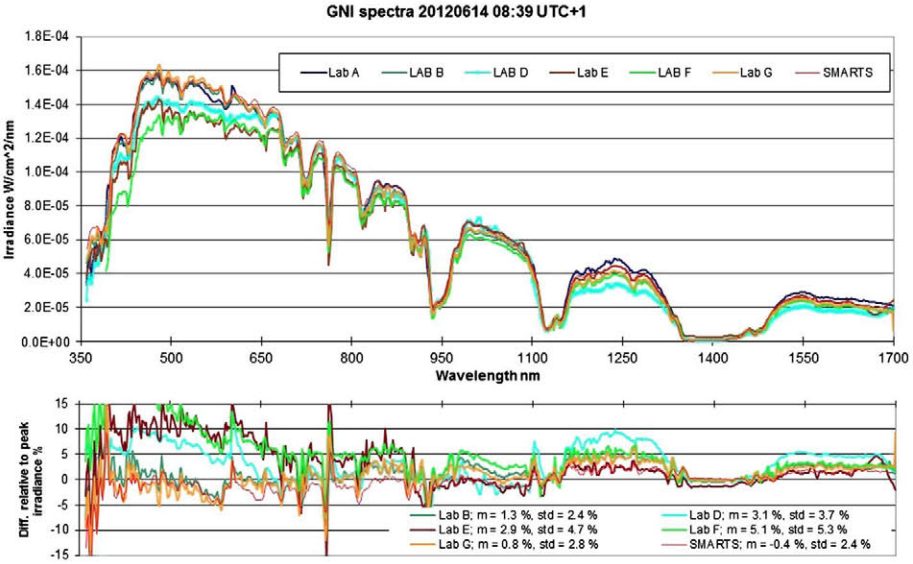

Figure 4. *Upper*: six GNI measured spectra plus spectrum obtained from the same time period by SMARTS code. *Lower*: wavelength-by-wavelength difference with respect to the Lab A spectrum and normalized to its peak irradiance; average and standard deviation calculated over the interval 360–1700 nm are also reported.

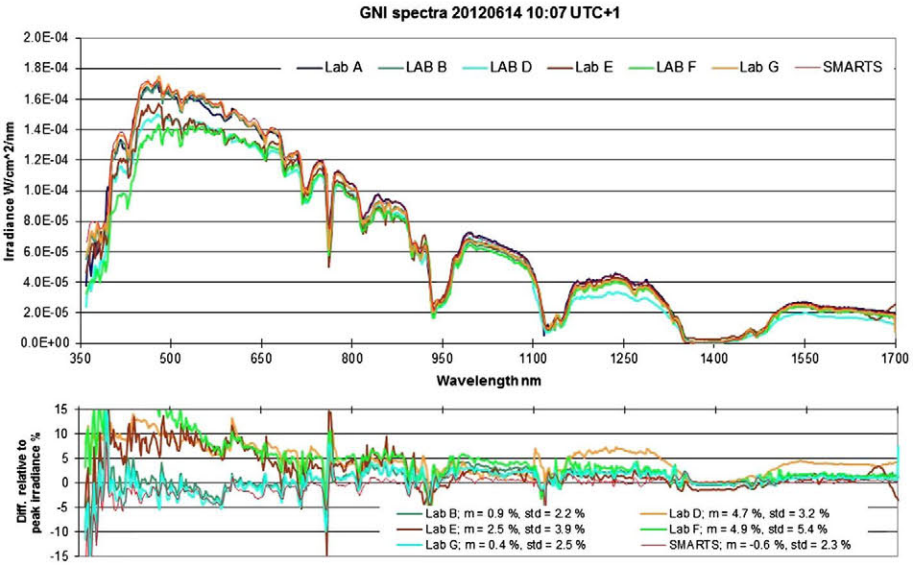

Figure 5. *Upper*: six GNI measured spectra plus spectrum obtained from the same time period by SMARTS code. *Lower*: wavelength-by-wavelength difference with respect to the Lab A spectrum and normalized to its peak irradiance; average and standard deviation calculated over the interval 360–1700 nm are also reported.

3.2. Integrated GNI, DNI irradiance data versus cavity radiometer and shadowed pyranometer data

A further data analysis performed on the acquired solar spectra was to compare the irradiance obtained by integrating the measured spectra versus the actual irradiance measured by cavity radiometers plus, in case of GNI, shaded pyranometers. This may be of interest because secondary laboratories use to derive from spectroradiometer measurements both relative solar spectral- and total-irradiance information. Measured GNI and DNI data were suitably reduced to account for the different spectral sensitivity between spectroradiometers and broadband radiometers. Measured irradiance data were reduced to a fraction equal to the irradiance fraction of the corresponding wide-band (300–4000 nm) SMARTS spectra, falling into the wavelength band 360–1700 nm. No corrections for

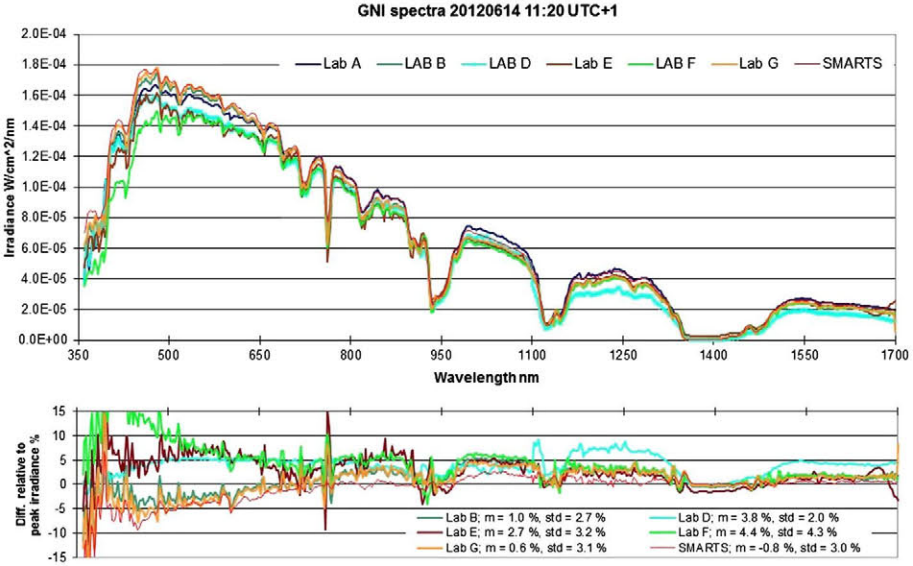

Figure 6. *Upper*: six GNI measured spectra plus spectrum obtained from the same time period by SMARTS code. *Lower*: wavelength-by-wavelength difference with respect to the Lab A spectrum and normalized to its peak irradiance; average and standard deviation calculated over the interval 360–1700 nm are also reported.

difference in the instruments viewing angle were applied. Table II reports the average differences between GNI irradiance values, as calculated by integrating spectral irradiance graphs, and the corresponding measured irradiance values obtained by cavity radiometer plus diffused pyranometer data. Reported average values refer to 20 GNI spectra acquired during a half day measurement session. Moreover, GNI values that result by integrating SMARTS spectra in the 360–1700 nm band are also shown for consistency check. Modeled spectra were obtained using actual local measurement time, temperature, atmospheric pressure, relative humidity and terrain type as input parameters. Figure 7 graphically shows the time evolution of the data summarized in Table II. All GNI values obtained by integrating spectroradiometers' data are lower than the corresponding values measured by cavity plus shaded pyranometer. Differences range from almost zero to −11.2%; all but one value in Table II have associated standard deviation below 1% suggesting systematic and uniform irradiance underestimation as confirmed by the smooth trend of most of the plots reported in Figure 7. A similar analysis was performed also on a set of spectral DNI acquisition. In this case, the integral irradiance data were compared with the simultaneous values measured by the cavity radiometer only; in analogy to the previous GNI case, cavity-measured irradiance data were duly reduced to account for difference in measurement spectral bandwidth among cavity radiometers and spectroradiometers. Figure 8 reports the time evolution for integrated versus cavity-measured percentage difference during a spectral DNI acquisition session. Averages of data shown in Figure 8 are summarized in Table III.

Table II. Average difference values, expressed in percent, between calculated and measured global normal incidence irradiance for a group of 20 spectra measured by each partner.

Laboratory	Average difference %	Standard deviation %
Lab A	−0.1	0.8
Lab B	−2.7	0.3
Lab D	−10.3	1.7
Lab E	−6.8	0.5
Lab F	−11.2	0.7
Lab G	−1.5	0.2
SMARTS	1.4	0.5

These results show all that but one laboratory underestimate actual irradiance with differences up to −8.6%. Excluding data from Lab F, each laboratory has consistent DNI and GNI average differences within the associated standard deviation shown in Tables II and III. However, data in Table III show larger standard deviations as highlighted by the non-uniform trend and missing points of some plots in Figure 8. A missing measurement point in Figure 8 denotes that the relevant instrument had an unstable or false measurement, that it was not measuring because performing a zeroing (e.g. dark current) or it was off line for optical re-alignment.

4. IMPACT OF USING SPECTRA MEASURED BY DIFFERENT INSTRUMENTS ON PV DEVICE CALIBRATION

How the differences in measured spectra may affect the PV device calibration activities is an interesting outcome of

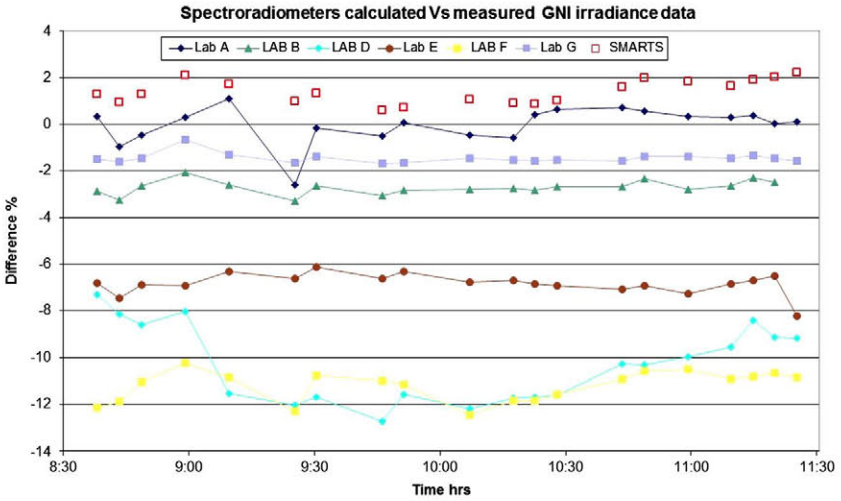

Figure 7. Time evolution of the integrated versus cavity plus shaded pyranometer measured irradiance data during a spectral GNI measurement session.

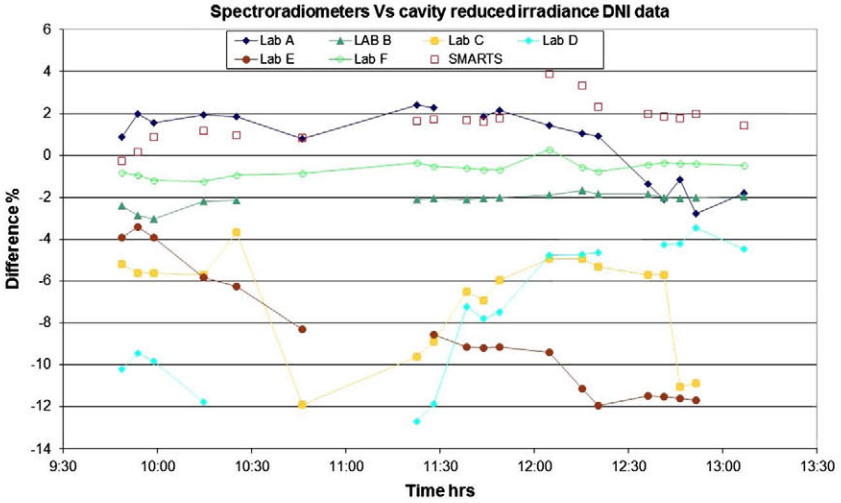

Figure 8. Evolution of the integrated versus cavity-measured irradiance data during a spectral DNI measurement session. Discontinuity in the line connecting data points highlights missing measurement points.

this intercomparison exercise. The calibration of a generic PV cell at standard test conditions (STC) entails the correction of its measured short circuit current (I_{sc}) from the actual irradiance, temperature and spectrum data to 1000 W/m^2, 25 °C and AM1.5 standard spectrum, respectively [7,8]. The correction to AM1.5 standard spectrum (either direct for CPV or global for flat panels) is performed by applying to the measured I_{sc} a spectral mismatch correction factor (SMM) described in Equation 1. In primary PV device calibration, the reference detectors are a cavity radiometer (for measuring direct irradiance) together with a diffuse pyranometer (to obtain global irradiance). Both of the instruments mentioned previously are supposed to have a wavelength independent spectral responsivity, and hence, their contribution does not appear in the right hand side of Equation (1):

$$SMM = \frac{\int SR_{dut}(\lambda)E_{ref}(\lambda)d\lambda}{\int SR_{dut}(\lambda)E_{meas}(\lambda)d\lambda}\frac{\int E_{meas}(\lambda)d\lambda}{\int E_{ref}(\lambda)d\lambda} \quad (1)$$

where $SR_{dut}(\lambda)$ is the spectral responsivity of the considered device, and $E_{ref}(\lambda)$ and $E_{meas}(\lambda)$ are the spectral irradiance of Air Mass 1.5 standard spectrum (either direct or global) and of measured spectrum, respectively. The SMM correction factor accounts for the difference between the actual spectrum under which the calibration

Table III. Average difference values, expressed in percent, between calculated and measured DNI irradiance.

Laboratory	Average difference %	Standard deviation %
Lab A	0.7	1.7
Lab B	−2.1	0.3
Lab C	−6.9	2.5
Lab D	−7.4	3.2
Lab E	−8.6	3.0
Lab F	−0.6	0.4
SMARTS	1.6	1

was performed and the reference AM1.5 spectrum [9]. During the spectroradiometer comparison, a set of Iso-Type cells equipped with collimating tubes and whose spectral response is shown in Figure 9, had their I_{sc} measured and calibrated to STC applying SMM values calculated from, approximately, 20 DNI spectra per partner. The use of Iso-Type cell allows isolating three bands of the spectrum corresponding to the spectral responsivity of each cell and, therefore, increasing the quantity of information. However, in the calibration of a triple-junction cell, where all sub-cells are series connected, only the limiting junction, top or middle sub-cell, is determining the cell overall current. The exercise involving DNI spectra is a worst case scenario as the intercomparison results for spectral DNI gave larger discrepancies among partners. The voltages measured across each cell's shunt were previously converted to current and, then, linearly corrected to 1000 W/m^2 using irradiance data by a cavity radiometer. The last step in the calibration procedure entails the correction for the spectral mismatch between actual and reference spectra using MMFs obtained applying Equation (1). The comparison of the I_{sc} values at STC gives also a figure of the calibration equivalence among participating laboratories. Table IV summarizes for each Iso-Type cell the average I_{sc} corrected to STC value for each partner, the associated standard deviation and the percentage deviation from the value $\overline{I}_{sc}$ obtained as weighted average of all partners I_{sc}. $\overline{I}_{sc}$ was computed applying Equation (2).

$$\overline{I}_{sc} = \frac{\sum_{i=1}^{6}(x_i w_i)}{\sum_{i=1}^{6} w_i} \tag{2}$$

where x_i is the I_{sc} average value for each partner and w_i is the inverse of its associated variance. I_{sc} calibration values from all partners lay in a band of ±7.5%, ±2% and ±12% from $\overline{I}_{sc}$ for Top, Middle and Bottom cell, respectively. A restricted group of four laboratories (Labs A, B, E and F) show I_{sc} values in agreement to each other within ±4.4%, ±1% and ±7% for Top, Middle and Bottom cell, respectively.

These results reflect the differences in the shape of the measured spectra within the responsivity band of the considered cell. Looking at Figures 1–3, which represent three of the measurements used for the calibration exercise, the reported spectra show a better agreement in the wavelength interval corresponding to the responsivity of the middle cell (650–900 nm). On the other hand, the wavelength interval corresponding to the spectral responsivity of the bottom cell, 900 nm onward, shows large instability and artifacts, resulting in important deviations in MMF among partners. In a previous work [3], a simulation exercise using a c-Si reference cell and two measured spectra with substantial differences in the 300–400 nm region and above 850 nm showed a 2% difference in the I_{sc} values when corrections for the spectral mismatch were applied.

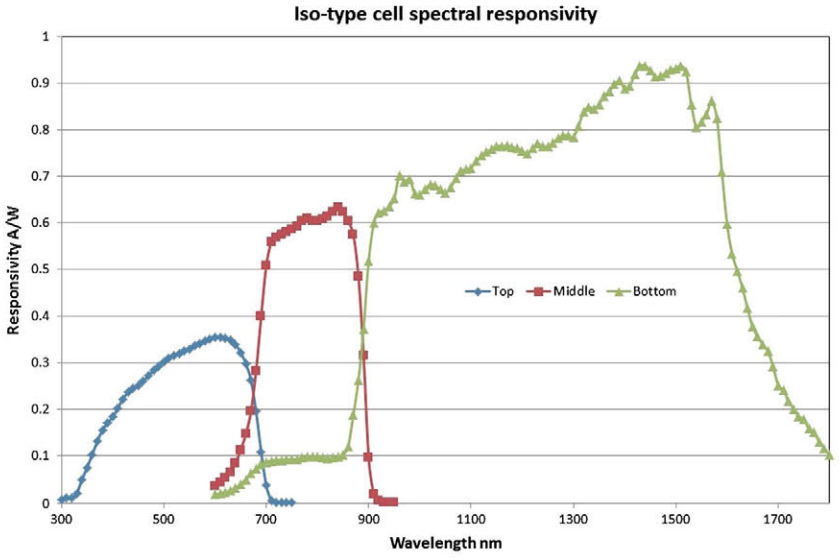

Figure 9. Spectral responsivity of the Iso-type cells used in the calibration exercise.

Table IV. Average of the short circuit current calibration values (I_{sc} values corrected at STC) for three Iso-type cells applying spectral mismatch correction factors derived from simultaneously measured DNI spectra.

	Cal value *Top* (mA)	Std dev %	Cal value versus $\bar{I}_{sc}$ (%)	Cal value *Middle* (mA)	Std dev %	Cal value versus $\bar{I}_{sc}$ (%)	Cal value *Bottom* (mA)	Std dev %	Cal value versus $\bar{I}_{sc}$ (%)
Lab A	1.46	1.3	4.4	1.43	0.7	−0.9	2.53	1.5	−5.5
Lab B	1.40	0.3	−0.4	1.45	0.3	0.2	2.68	0.2	0.3
Lab C	1.33	3.1	9.0	1.41	2.6	0.9	2.97	8.0	−16.1
Lab D	1.53	1.9	−5.4	1.46	2.3	−2.5	2.24	4.5	11.2
Lab E	1.35	2.1	−3.9	1.42	1.2	−1.6	2.90	4.6	8.5
Lab F	1.41	0.3	0.2	1.45	0.3	0.1	2.65	0.3	−0.7

Per cent difference to the weighted average calibration value $\bar{I}_{sc}$ is reported for each cell and laboratory.

5. CONCLUSION AND DISCUSSION

An intercomparison of spectroradiometers for global and direct normal incidence irradiance in the visible and near infrared spectral regions, together with the assessment of the impact its results may have on the spectral mismatch calculation of a triple-junction PV device, was performed. Six European scientific laboratories and a Japanese industrial partner were involved in the intercomparison for a total of seven spectroradiometer systems covering the wavelength range from 360 to 1700 nm. Because of the different technologies of the involved instruments, specific timing and measurement procedure, and irradiance stability criteria have been developed in order to make meaningful data comparison.

From the result analysis of spectral DNI measurements, the wavelength-by-wavelength percentage spectra difference normalized to peak spectral irradiance and averaged in the 360–1700 nm interval remains below 6%. For restricted wavelength regions, differences remain, in general, in a band of −5% to 10% with a single partner exceeding 15%. The same analysis on GNI spectra showed an average wavelength-by-wavelength value not exceeding 5.1%. Three instruments (Lab A, Lab B and Lab G) have all points of GNI spectra laying in a band of ±5%. Comparison of DNI data calculated by integrating the spectra curves versus DNI values derived by cavity radiometer measurements showed average deviations ranging from +0.7% to −8.6%. Cavity-measured irradiance values were corrected to account for spectroradiometers' narrower bandwidth. A similar analysis performed on a set of GNI spectra versus cavity radiometer plus shaded pyranometer measurements showed deviation ranging from −0.1% to −11.2%. A set of Iso-Type cell was calibrated during the intercomparison, and the spectral mismatch factors derived from each partner measured spectra were used for the I_{sc} correction at STC of each cell. The spread of the resulting calibration values for the four laboratories with the lower associated standard deviations was found to be within ±4.4%, ±1% and ±7% for Top, Middle and Bottom cell, respectively.

These results represent an important element to assess the calibration equivalence among laboratories. The aforementioned spread results for Top and Bottom cells are in agreement with previously published calibration round robin results both for c-Si modules [10,11], laying in the ±3% range, and cell [12,13] where the best agreement is in the ±1% range. Moreover, the I_{sc} calibration exercise results are an experimental confirmation of previously performed simulations on the results of the first spectroradiometers comparison campaign [3].

REFERENCES

1. Martínez-Lozano JA, Utrillas MP, Pedrós R, Tena F, Díaz JP, Expósito FJ, Lorente J, de Cabo X, Cachorro V, Vergaz R, Carreño V. Intercomparison of spectroradiometers for global and direct solar irradiance in the visible range. *Journal of Atmospheric and Oceanic Technology* 2003; **20**: 997–1010.
2. Krawczynski M, Strobel MB, Gottschalg R. Intercomparison of spectroradiometers for outdoor performance monitoring Proceedings of the 24th European Photovoltaic Solar Energy Conference, 21-25 September 2009, Hamburg, Germany.
3. Galleano R, Zaaiman W, Virtuani A, Pavanello D, Morabito P, Minuto A, Spena A, Bartocci S, Fucci R, Leanza G, Fasanaro D, Catena M. Intercomparison campaign of spectroradiometers for a correct estimation of solar spectral irradiance: results and potential impact on photovoltaic devices calibration. *Progress in Photovoltaics: Research and Applications* 2013. DOI: 10.1002/pip.2361
4. IOM report No. 91 WMO/TD No. 1320, 2006; http://www.pmodwrc.ch/pdf/ipc-x_final.pdf
5. Gueymard C. Parameterized transmittance model for direct beam and circumsolar spectral irradiance. *Solar Energy* 2001; **71**(5): 325–346.
6. Gueymard C. SMARTS, a simple model of the atmospheric radiative transfer of sunshine: algorithms and performance assessment. Professional Paper FSEC-PF-270-95. Florida Solar Energy Center, 1679 Clearlake Rd., Cocoa, FL 32922, 1995.

7. ISO-IEC 60904-3 Photovoltaic devices—Part 3: measurement principles for terrestrial photovoltaic (PV) solar devices with reference spectral irradiance data. International Organization for standardization, Geneva, Switzerland, www.iec.ch
8. ISO-IEC 60904-4 Photovoltaic devices—Part 4: reference solar devices—procedures for establishing calibration traceability. International Organization for standardization, Geneva, Switzerland, www.iec.ch
9. Muellejans H, Ioannides A, Kenny R, Zaaiman W, Ossenbrink H, Dunlop E. Spectral mismatch in calibration of photovoltaic reference devices by global sunlight method. *Measurement Science and Technology* 2005; **16**: 1250–1254. DOI: 10.1088/0957-0233/16/6/002
10. Betts TR, Zdanowicz T, Prorok M, Kolodenny W, de Moor H, Borg N, Stellbogen D, Hohl-Ebinger J, Warta W, Friesen G, Chianese D, de Montgareu AG, Herrmann W, Berrade JD, Moracho J, Cueli AB, Lagunas AR, Gottschalg R. Photovoltaic performance measurements in Europe: PV-Catapult Round Robin Tests, Conference Record of the 2006 IEEE 4th World Conference on Photovoltaic Energy Conversion, Vol. 2, Hawaii, 2006.
11. Rummel S, Anderberg A, Emery K, King D, TamizhMani G, Arends T, Atmaram G, Demetrius L, Zaaiman W, Cereghetti N, Herrmann W, Warta W, Neuberger F, Morita K, Hishikawa Y. Results from the second international module inter-comparison, Conference Record of the 2006 IEEE 4th World Conference on Photovoltaic Energy Conversion, Vol. 2, Hawaii, 2006.
12. van der Heide A, Winter S, Moriarty T, Zaaiman W. Comparison between large references cells calibrated by ESTI-JRC, NREL and PTB, performed at ECN, Conference record of 20th European Photovoltaic Solar Energy Conference, 6-10 June 2005, Barcelona, Spain
13. Winter S, Metzdorf J, Emery K, Fabero F, Hishikawa Y, Hund B, Mullejans H, Sperling A, Warta W. The results of the second World Photovoltaic Scale recalibration Conference Record of the Thirty-first IEEE Photovoltaic Specialists Conference, 2005. DOI: 10.1109/PVSC.2005.1488304